Hydrogen-Bonding Density of Supramolecular Self-Assembled Fibrillar Networks Probed Using Synchrotron Infrared Spectromicroscopy

ARTICLE *in* CRYSTAL GROWTH & DESIGN · AUGUST 2009

Impact Factor: 4.89 · DOI: 10.1021/cg900370g

3 AUTHORS, INCLUDING:

Michael A Rogers
University of Guelph
65 PUBLICATIONS **1,061** CITATIONS
SEE PROFILE

Luca Quaroni
Institute of Nuclear Physics
84 PUBLICATIONS **1,017** CITATIONS
SEE PROFILE

CRYSTAL GROWTH & DESIGN
XXXX
VOL. XXX, NO. XX

Hydrogen-Bonding Density of Supramolecular Self-Assembled Fibrillar Networks Probed Using Synchrotron Infrared Spectromicroscopy

Michael A. Rogers,*[,†] Tor Pedersen,[‡] and Luca Quaroni[‡,§]

Department of Food and Bioproduct Sciences, University of Saskatchewan, Saskatoon, Saskatchewan S7N5A8, Canada, Canadian Light Source, Saskatoon, Saskatchewan S7N0X4, Canada, and Department of Chemistry, University of Manitoba, Winnipeg R3T 2N2, Canada

Received April 3, 2009; Revised Manuscript Received June 1, 2009

ABSTRACT: We employed synchrotron infrared spectromicroscopy to provide new insights into the development of self-assembled fibrillar networks. The noncovalent interactions responsible for the occurrence of transient junction zone in 12HSA arise because of hydroxyl−hydroxyl hydrogen bonding. This may result from the preferential arrangement of carboxylic acid groups to dimerize within the fiber, resulting in a reduction of the fiber−solvent interfacial tension. As well, synchrotron infrared spectromicroscopy indicates that the crystallization process of SAFiNs efficiently displaces solvent from the interface of the growing crystals contributing to the epitaxial growth into axially symmetric elongated aggregates. The periodicity in the density of hydrogen bonding resolves the supramolecular chirality of 12HSA fibers.

Introduction

Self-assembled fibrillar networks (SAFiNs) have renewed interest in the food,[1,2] cosmeceutical, pharmaceutical,[3] and petrochemical industries.[4] Numerous potential applications are feasible by result of their vast diversity in terms of microscopic and mesoscopic structures.[5] The food industry is investigating the potential for organogels to structure edible polyunsaturated oils, thereby reducing the need for heart-unhealthy lipids including saturated and trans fats.[2] The cosmetic and pharmaceutical industries are developing this technology for topical applications in drug and cosmeceutical delivery.[3] In this instance, the rate of delivery is governed by the pore size distribution within the gel network, thus creating a need to develop an understanding of the nanostructure.[6−8] Furthermore, SAFiNs are present in unique materials found in nature including naturally occurring silk, collagen, and clathrin as well as pathological fibers such as amyloid plaques.[9−11] The potential of SAFiNs as novel soft materials has been underutilized thus far, on account of the inability to understand how supramolecular structures develop nanofibers comprising low-molecular-weight organogelators interacting via noncovalent interactions.[12]

Molecular gels require small molecular weight gelators to noncovalently interact, forming nanofibers preceding supramolecular network formation. Cooling the organogelator−solvent melt below the melting point of the organogelator forms a supersaturated state, causing gelator molecules to microscopically phase separate and self-assemble via stochastic nucleation events driven by enthalpic forces.[13] Unlike most hydrogels, which are driven to aggregate by hydrophobic attractions or are entropically driven,[5] nanofibers characteristically are enthalpically driven. This causes gelator molecules to aggregate forming a network of rods, tubes, or sheets formed primarily via noncovalent interactions including hydrogen bonding, van der Waals interactions, $\pi-\pi$ stacking, and metal coordination.[14] The ability for SAFiNs to self-assemble into rodlike structures requires a careful balance involving the contrasting parameters of solubility and the parameters controlling epitaxial growth.[13,14]

SAFiNs contain fibers of varying lengths and thicknesses depending on the crystal history and the types of junction zones present (i.e., transient and/or permanent).[12] Transient or nonpermanent junction zones occur between individual fibers of 12HSA in apolar solvents and typically result in the formation of weak gels.[5] Nonpermanent interactions are subject to the nature and polarity of the solvent which may either promote or interfere with fiber−fiber interactions. Permanent junction zones are more effective at entraining the liquid apolar phase in the resulting meshlike network.[15] The permanent junction zones arise because of crystallographic mismatches at the interface of the growing one-dimensional crystals, resulting in branch points along the fibers.[12]

The ability of these small molecules to aggregate into rods, tubes or sheets via noncovalent interactions may be utilized to examine the nano and supramolecular structures of SAFiNs. Numerous functional groups are responsible for the noncovalent interactions characteristic of SAFiNs and have assignable absorption spectral features in the mid-infrared (mid-IR) region (4000−400 cm^{-1}) of the electromagnetic spectrum. Infrared spectroscopy has been utilized to study the noncovalent interactions relevant to each category of SAFiN, including steroid derivatives, anthryl derivatives, anthryl and anthraquinone appended steroid based gelators, organometallic gelators, and hydroxylated fatty acids. Steroid derivatives form chiral nematic liquid crystals[16] via noncovalent interaction between hydroxyl groups (3200 cm^{-1}) and $\pi-\pi$ stackings of the aromatic rings (3000−3100 cm^{-1}). The anthryl derivatives and the anthryl and anthraquinone appended steroid based gelators along with the organometallic gelators rely on multiple $\pi-\pi$ stacking (3000−3100 cm^{-1}).[17] Hydroxylated fatty acids rely on hydrogen bonding between the carboxylic acid groups (1700 cm^{-1}) and hydroxyl groups (3200 cm^{-1}).[7,8,18,19]

The use of a microscopy optical configuration allows IR absorption experiments on samples a few micrometers in size and has been used to study the properties of separate phases in heterogeneous mixtures. Conventional mid-IR spectromicros-

* Corresponding author. E-mail: michael.rogers@usask.ca. Tel: (306) 966-5028. Fax: (306) 966-8898.
† University of Saskatchewan.
‡ Canadian Light Source.
§ University of Manitoba.

10.1021/cg900370g CCC: $40.75

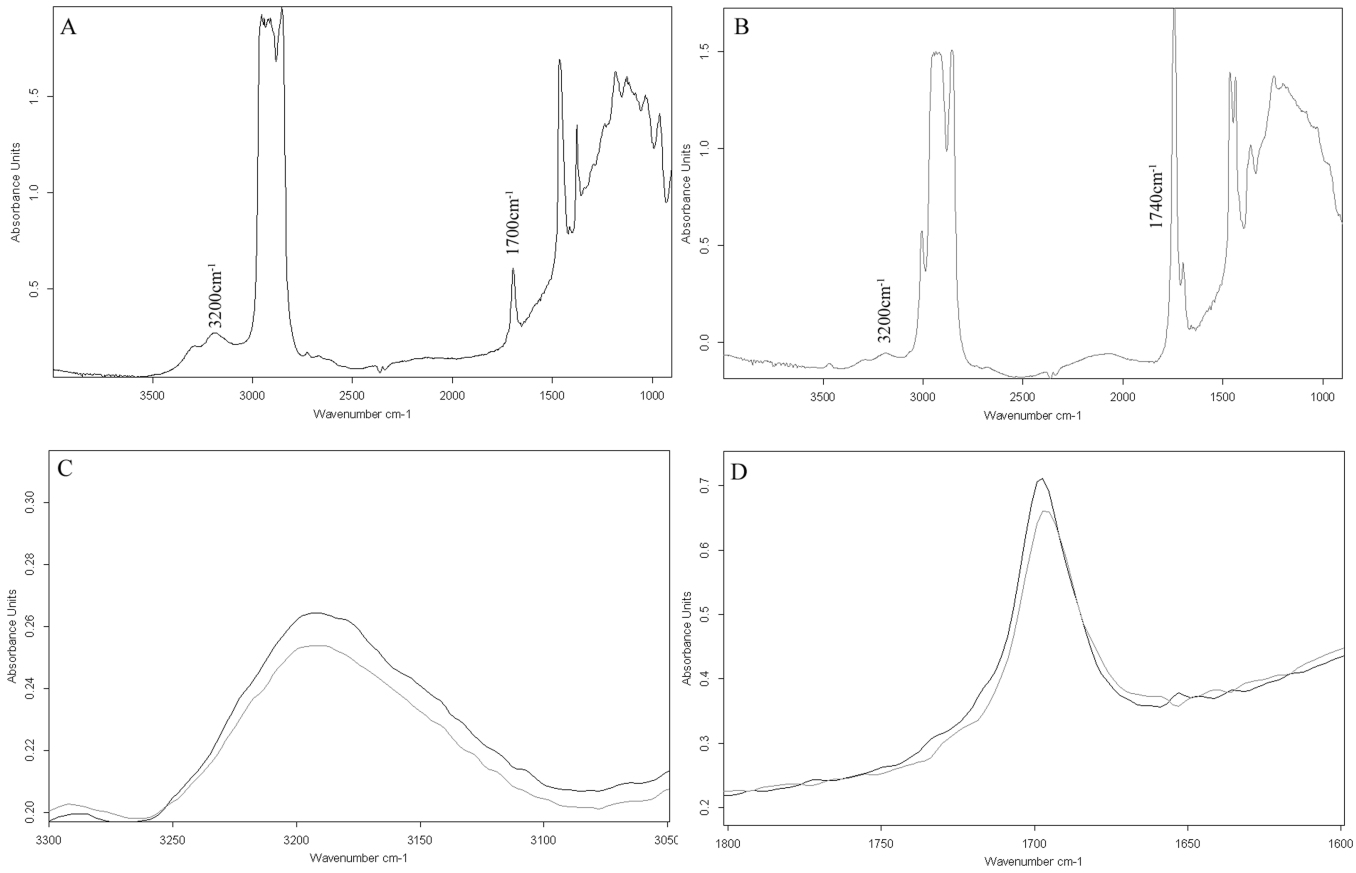

Figure 1. Fourier transform infrared spectrum of 12HSA in (A) mineral oil and (B) methyl oleate and the change in peak area of (C) the hydroxyl group peak at 3200 cm^{-1} and (D) the carboxylic acid band at 1700 cm^{-1}.

copy contends with constraints attributable to limited throughput, resulting in low signal-to-noise ratios when used with diffraction limited spatial resolution. This limitation can be overcome by using a brighter source of IR light obtained from synchrotron radiation, allowing the resolution and mapping of structural features at the diffraction limit, 3−15 μm in the mid-IR region.[20,21]

Thus, it is the purpose of this study to examine the distribution density of hydrogen bonding between carboxylic acid and hydroxyl groups within fibers as well as the hydrogen-bonding density resulting in fiber−fiber interactions using synchrotron infrared spectromicroscopy.

Methods

99% pure DL-12HSA was obtained from NuCheck Prep (Elysian, MN), methyl oleate and light mineral oil were obtained from Sigma Aldrich (Oakville, ON) and used as received. Two weight percent samples of 12HSA in each solvent were prepared by heating the mixture to 85 °C for 30 min. A drop of sample was placed between 2 mm thick CaF_2 25 mm diameter disks separated with a 15 μm Teflon spacer. The samples were then cooled on a Linkam L120 controlled temperature stage (Linkam, Surrey, United Kingdom) at 1 °C/min and were used for Fourier transform infrared spectroscopy (FTIR) mapping experiments on the endstation of the mid-IR beamline (beamline 01B1−01, Canadian Light Source, Saskatoon, SK). The endstation is comprised of a Bruker IFS66v/s interferometer coupled to a Hyperion 2000 IR microscope (Bruker Optics, Billerica, MA). Light is focused on the sample using a 36× magnification Schwarzschild condenser, collected by a 36× magnification Schwarzschild objective and detected by a liquid nitrogen cooled narrowband MCT detector with a 100 μm sensing element. Mapping was performed using a computer controlled Märzhäuser Wetzlar (Wetzlar, DE) stage using 5 μm increments in both the X and Y plane.

A KBr-supported Ge multilayer beamsplitter was used to measure spectra in the mid-infrared spectral region. Measurements were performed using Opus 6.5 software (Bruker Optics, Billerica, MA). Interferograms were collected using 256 scans and were recorded by scanning the moving mirror at 40 kHz, to an upper frequency limit of 7899 cm^{-1} and with a spectral resolution of 4 cm^{-1}. Single channel traces were obtained using the fast Fourier transform algorithm, without any zero-filling, after applying a Blackman-Harris 3-Term apodization function. For single spectra, measurements for reference single-channel traces the were carried out in air.

For the mapping experiments in Figure 2, absorption spectra were calculated by using a region devoid of crystalline material as the reference position and dividing every single-channel trace by the single-channel trace recorded in the reference position, to obtain transmittance spectra. These were then converted to absorbance spectra. Such procedure effectively provides spectra that represent differences in absorbance relative to the reference position. The absorbance changes were represented as two-dimensional maps of the sample, where each point represents the absorbance value at a given frequency or the area of the difference absorption band observed at that frequency. During these experiments, care was taken to place the lower left corner of the mapped area in a position that appeared devoid of any crystalline formations. Therefore, for all maps reported in this work, the $X = 0$ and $Y = 0$ position were used as the reference position.

Results and Discussion

It has been well-established that there are two types of junction zones: permanent and transient. Permanent junction zones arise from crystallographic mismatches disrupting the crystalline order of the growing crystal interface resulting in the formation of a branched fiber.[12] The supersaturation-driven crystallographic mismatch branching (also called noncrystallographic branching) is governed by the nucleation and growth kinetics of the gel network.[12] These permanent junction zones

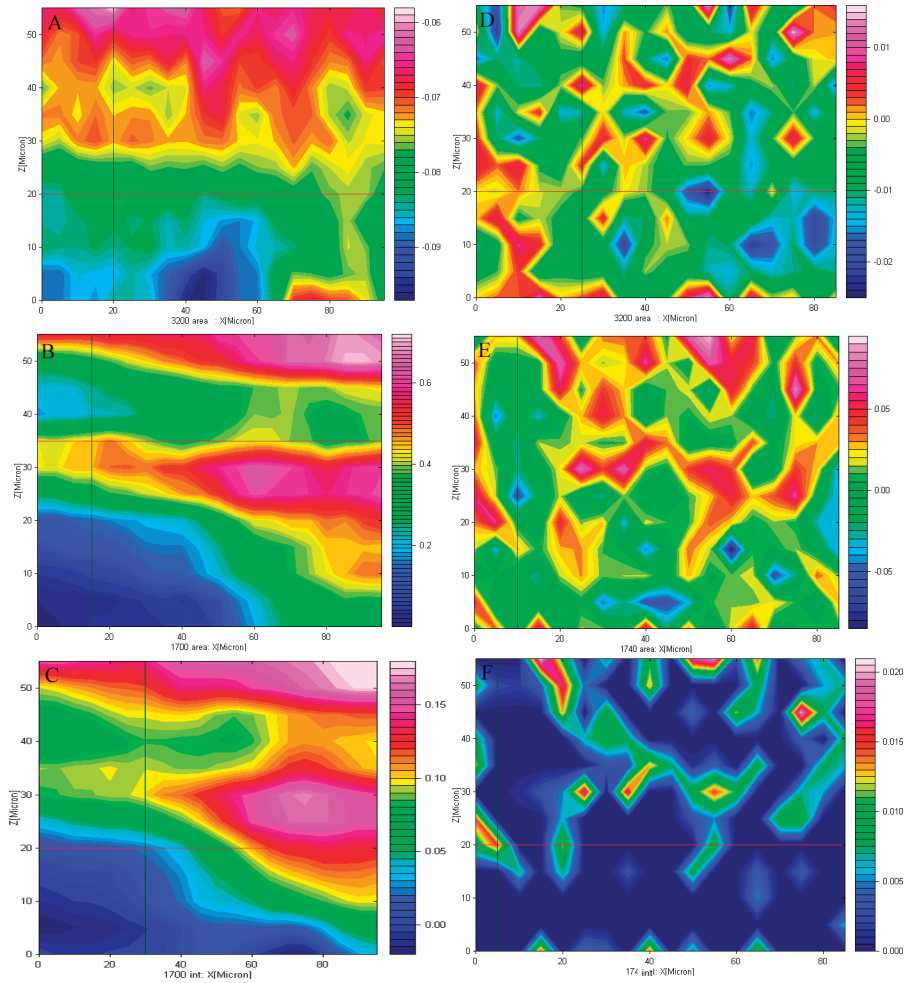

Figure 2. Fourier transform infrared maps of the relative change in (A, D) hydroxyl hydrogen-bonding area, (B) carboxylic acid dimerization area, (C) carboxylic acid dimerization intensity, (E) ester band area, and (F) intensity for mineral oil (A−C) and methyl oleate (D−F).

are in part responsible for the elastic nature of these soft materials as well as their ability to retain the liquid apolar phase.[7,8] As well, transient junction zones play a crucial role in the oil mobility as well as the elastic component. The nonpermanent interactions between fibers are often overlooked and in many cases may be oversimplified. Typically, it is believed that nanofibers assemble via hydrogen bonding while interactions between nanofibers results from van der Waals interactions.[14] However, with all the works on the supramolecular interactions between SAFiNs there are several postulations on how these fibers interact to form three-dimensional networks. Using synchrotron infrared spectromicroscopy, we measured the interactions within and between the fibers directly.

Synchrotron infrared spectromicroscopy was used to determine the prevalence of hydrogen bonding in two SAFiN systems: 12HSA in mineral oil and 12HSA in methyl oleate. Nanofibers of 12HSA develop due to the dimerization of carboxylic acid groups and longitudinal growth occurs via hydrogen bonding between hydroxyl groups.[18] As a result of these structural features, two spectral elements may be observed. Dimerization of carboxylic acids can be monitored at 1700 cm^{-1},[19,29] whereas hydrogen bonding between hydroxyl groups can be monitored by an increase in area of the broad peak at 3200 cm^{-1}.[29] Hence, for 12HSA in mineral oil, the bands monitored correspond to the hydroxyl groups and the carboxylic acid groups (Figure 1A). Using 12HSA in methyl oleate, a new spectral feature at 1740 cm^{-1} is evident because of the ester bond in methyl oleate (Figure 1B).[26] Two absorbance spectra were used to illustrate the change in absorbance for the hydroxyl groups (Figure 1C) and the carboxylic acid groups (Figure 1D). The major disadvantage of the 12HSA in methyl oleate is the ester band overlaps the spectral feature arising from the dimerization of the carboxylic acid groups. This inhibits its resolution allowing for only the hydroxyl interactions on the 12HSA molecule to be monitored. However, the ester band was also mapped to observe if areas concentrated in SAFiN hydroxyl hydrogen bonding are depleted of the solvent spectral features corresponding to the ester band.

For 12HSA in mineral oil, the area of the peak at 3200 cm^{-1}, corresponding to the hydroxyl−hydroxyl interactions between molecules (Figure 2A), and the area (Figure 2B) and intensity (Figure 2C) of the dimerization of carboxylic acid groups on 12HSA at 1700 cm^{-1} were mapped. The two-dimensional maps for 12HSA/mineral oil revealed two distinct fibers with an approximate width of ∼8−10 μm. The width corresponds well with previously obtained cryo-SEM images.[23] Figure 2A−C present the same field-of-view and are superimposable.

Strands of 12HSA have a helical nature because of the supramolecular arrangement of fibers arising from the chirality at position 12 on 12HSA.[22−27] Previously, 12HSA strands in mineral oil where shown to be approximately 100 μm long and 3−8 μm wide.[28] However, for methyl oleate, the fibers range greatly in length from 5 to 75 μm and are approximately the same width as observed in mineral oil.[28] The supramolecular

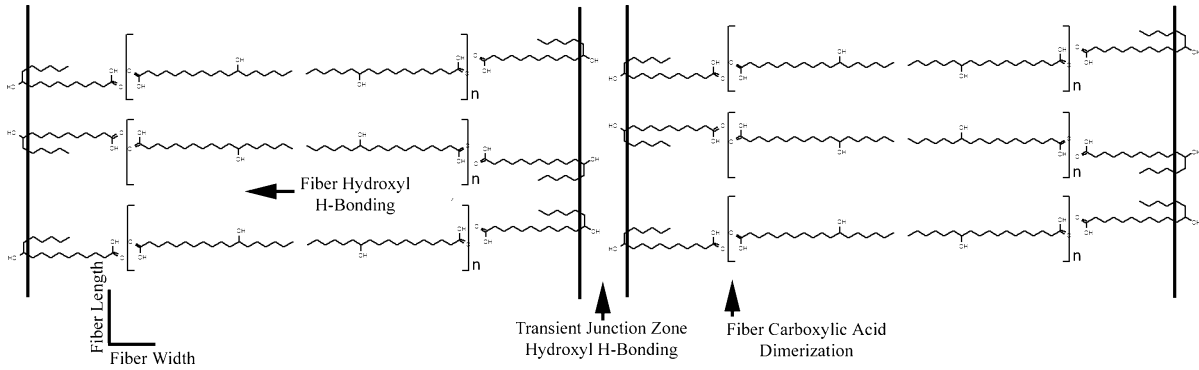

Figure 3. Representation of the structure of 12HSA network formation corresponding to the spectral features measured using FTIR.

helical configuration instilled from the chiral carbon may be observed via the hydrogen bonding periodicity within the fibers illustrated by the reddish-pink zones containing concentrated dimerization in the crystalline structure (Figure 2B).

These two individual fibers present in mineral oil where observed by monitoring both the area (Figure 2B) and intensity (Figure 2C) of the carboxylic acid interactions. Figure 2B and C indicates a reduction in the amount of COOH−COOH interactions between fibers suggesting that upon formation of the crystalline supramolecular helix these groups are effectively excluded from the fiber−solvent interface thereby reducing the fiber-solvent interfacial tension. Figure 2A indicates that the fibers' nonpermanent junction zones interact via hydrogen bonding of the hydroxyl groups while preferentially excluding the carboxylic acid groups from the surface of the fiber. As a result, the hydroxyl groups at position 12 are exposed to the surface, which is illustrated in Figure 3. During the development of SAFiNs, certain groups capable of hydrogen bonding are selectively buried, which may result in other functional groups being exposed at the interface. In the case of 12HSA, carboxylic acid groups are preferentially buried and hydroxyl groups are exposed. The idea that nanofibers interact to form the supramolecular network via van der Waals interactions alone, in certain cases, may be oversimplified.

12HSA in methyl oleate produced very few long fibers resulting in small densely packed crystals (Figure 2D) corresponding to the spectral features observed in Figure 2E. Both images illustrate that numerous 5−10 μm crystals are present. The size of these crystals is close to the diffraction limit of resolution for mid-IR radiation and is of the order of the step of the mapping stage. Therefore most of the crystals appear as one or two pixels in the IR maps. The areas elevated in hydroxyl−hydroxyl interactions (Figure 2D, reddish nuclei) correspond to the areas depleted of the ester band for methyl oleate (Figure 2E,F, blue solvent), suggesting that the development of 12HSA fibers is extremely efficient at displacing the solvent from the growing fiber surface and as a result develops densely packed crystals. However, numerous other crystallization processes, as in the case of triacylglyceride (TAGs), often entrain liquid TAGs during the formation of large diffusion limited clusters. It is also observed that even though these crystals appear as distinct structural elements, hydrogen-bonding intensities (Figure 2D) suggest that there is some level of noncovalent interactions between crystals forming a continuous network capable of entraining the liquid oil via transient junction zones.

Conclusions

Synchrotron infrared spectromicroscopy provides valuable information when mapping noncovalent interactions within SAFiNs. The supramolecular development of self-assembled fibers relies on noncovalent interactions to stabilize both the crystalline fibers and the transient and permanent junction zones between adjacent fibers. Direct evidence is provided indicating that fibers do not necessarily interact via van der Waals interactions alone but have significant hydrogen bonding occurring between fibers. For 12HSA in mineral oil fiber−fiber transient junction zones are stabilized by interactions between hydroxyl groups exposed at the fiber−solvent interface. Furthermore, the crystallization process of SAFiNs efficiently displaces solvent from the interface of the growing crystals contributing to the epitaxial growth into axially symmetric elongated aggregates.

Acknowledgment. The research described in this paper was performed at the Canadian Light Source, which is supported by NSERC, NRC, CIHR, and the University of Saskatchewan. The authors are grateful to Tim May (CLS) for beamline design, construction, and constant help in beamline upkeep. This project was supported by the National Science and Engineering Research Council of Canada (NSERC) Discovery Program.

References

(1) Rogers, M. *Food Res. Int.* **2008**, *42*, 747.
(2) Pernetti, M.; van Malssen, K. F.; Floter, E.; Bot, A. *Curr. Opin. Colloid Interface Sci.* **2007**, *12*, 221.
(3) Vintiloiu, A.; Leroux, J.-C. *J. Controlled Release* **2008**, *125*, 179.
(4) Battacharya, S.; Krishnan-Ghosh, Y. *Chem. Commun.* **2001**, 185.
(5) Terech, P.; Weiss, R. G. *Chem. Rev.* **1997**, *97*, 3133.
(6) Kantaria, S.; Rees, G. D.; Lawrence, M. J. *J. Controlled Release* **1999**, *60*, 355.
(7) Rogers, M. A.; Wright, A. J.; Marangoni, A. G. *Curr. Opin. Colloid Interface Sci.* **2009**, *14*, 33.
(8) Rogers, M. A.; Wright, A. J.; Marangoni, A. G. *Soft Matter* **2008**, *4*, 1483.
(9) Jin, H.-J.; Kaplan, D. L. *Mech. Nat.* **2003**, *424*, 1057.
(10) Lui, W.; Prausnitz, J. M.; Blanch, H. W. *Biomacromolecules* **2004**, *5*, 1818.
(11) Kirchhausen, T. *Ann. Rev. Biochem.* **2000**, *69*, 699.
(12) Wang, R.; Lui, X.-Y.; Xiong, J.; Li, J. *J. Phys. Chem. B* **2006**, *110*, 7275.

(13) Weiss, R. G.; Terech, P. *Molecular Gels Materials with Self-Assembled Fibrillar Networks*; Springer: Dordrecht, The Netherlands, 2007.
(14) Suzuki, M.; Nakajima, Y.; Yumoto, M.; Kimura, M.; Shirai, H.; Hanabusa, K. *Langmuir* **2003**, *19*, 8622.
(15) Liu, X. Y. *Top. Curr. Chem.* **2005**, *256*, 1.
(16) Ramanathan, N.; Currie, A. L.; Ross Colvin, J. *Nature.* **1961**, *190*, 779.
(17) Terech, P.; Desvergnes, J. P.; Bouas-Laurent, H. J. *J. Colloid Interface Sci.* **1995**, *174*, 258.
(18) Kuwahara, T.; Nagase, H.; Endo, T.; Ueda, H.; Nakagaki, M. *Chem. Lett.* **1996**, 435.
(19) Rogers, M. A.; Marangoni, A. G. *Cryst. Growth Des.* **2008**, *8*, 4596.
(20) Wright, A. J.; Marangoni, A. G. *J. Am. Oil Chem. Soc.* **2007**, *84*, 3.
(21) De Giacomo, O.; Cesàro, A.; Quaroni, L. *Food Biophys.* **2008**, *3*, 1557.
(22) Dumas, P.; Jamin, N.; Teillaud, J. L.; Miller, L. M.; Beccard, B. *Faraday Discuss.* **2004**, *126*, 289.
(23) Rogers, M. A.; Smith, A. S.; Wright, A. J.; Marangoni, A. G. *J. Am. Oil Chem. Soc.* **2007**, *84*, 899.
(24) Tachibana, T.; Kambara, H. J. *Colloid Interface Sci.* **1968**, *28*, 173.
(25) Uzu, Y.; Sugiura, T. *J. Colloid Interface Sci.* **1975**, *51*, 346.
(26) Fuhrhop, J.-H.; Schnieder, P.; Rosenberg, J.; Boekema, E. *J. Am. Chem. Soc.* **1987**, *109*, 3387.
(27) Terech, P.; Rodigues, V.; Barns, J. D.; McKenna, G. B. *Langmuir* **1994**, *10*, 3406.
(28) Rogers, M. A.; Marangoni, A. G. *Langmuir* **2009**, DOI: 10.1021/la8035665.
(29) Lin-Vien, D.; Colthup, N. B.; Fateley, W. G.; Grasselli, H. G. *The Handbook of Infrared and Raman Characteristic Frequencies of Organic Molecules*; Academic Press: New York, 1991.

CG900370G